

IDENTIFICATION OF CLAY MINERALS WITHIN THE SPRINGBOK FORMATION, SURAT BASIN

Mitchell Levy*

QUT

*Science and Engineering Faculty
GPO Box 2434, Brisbane, QLD, 4001
mitchell.levy@hdr.qut.edu.au*

Oliver Gaede

QUT

*Science and Engineering Faculty
GPO Box 2434, Brisbane, QLD, 4001
oliver.gaede@qut.edu.au*

SUMMARY

The Springbok Sandstone in the Surat Basin overlies the Walloon Coal Measures, an important coal seam gas resource. Here we investigate the hypothesis that potassium free or low-potassium clay minerals are the dominant clay minerals in the Springbok Sandstone, and review the effect this has on the ability of conventional well log analysis to successfully highlight high clay content rock units within the formation. Core samples from a test well have been analysed showing montmorillonite and kaolinite clays to be the dominant clay minerals within the formation.

Schlumberger Lithoscanner well log tool data from the test well has been compared to the laboratory core analysis revealing a good correlation between element concentrations identified by the tool and the laboratory data, however the mineralogy model which has been applied to this dataset does not appear to predict mineral assemblages within the formation successfully. Laboratory results have been compared to an existing conventional well log analysis for the basin, where gamma and density log cutoffs have been used to identify variations in lithology. Our investigation suggests this model does not successfully differentiate between clay rich and clay poor rocks within the Springbok Sandstone, and an alternative model using additional well logs is demonstrated to provide greater insight into lithology variations throughout the formation.

Key words: Surat, Springbok, Clay, Lithology, Coal Seam Gas

INTRODUCTION

The Walloon Coal Measures in the Surat Basin in Queensland are an important Coal Seam Gas resource. Development of this resource requires a thorough understanding of the surrounding lithologies. The Springbok Sandstone unconformably overlies the Walloon Coal Measures in a significant portion of the basin (Exon 1976). Despite the proximity of these two units there have been limited studies undertaken to understand the overall well log response of Springbok Sandstone, and in particular its clay phases.

The Surat Basin is a Jurassic to Lower Cretaceous aged sedimentary basin extending across approximately 300,000 km² through Southern Queensland and Northern New South Wales, unconformably overlying the permo-triassic Bowen Basin (Exon 1976, Hoffmann, et al. 2009). The basin is widely accepted to be an intracratonic sag basin, although the mechanisms for its formation are not completely resolved. Despite this, a general subsidence history and basin evolution are mostly agreed on in the literature (Hamilton, et al. 2014, Hodgkinson and Grigorescu 2012, Hoffmann, et al. 2009, Korsch and Totterdell 2009). The basin is dominated by large, laterally extensive units that can be broadly correlated across the basin. The dominant structure throughout the basin is the Mimosa Syncline, which trends approximately north-south centrally through the basin (Hodgkinson and Grigorescu 2012). The Springbok Sandstone has previously been classified as a generally permeable sandstone aquifer, however reported lithologies presented in the literature range across sandstones, mudstones, tuff, and coal layers (Exon 1976).

Gamma logs are often used in conventional well log analysis to differentiate broadly between so called ‘sand’ and ‘shale’ facies. Ellis (2007) describes shale in the context of well log analysis as being ‘fine-grained rock composed of silt and clay minerals’. Using gamma logs to differentiate between sand and shale relies on the shale having a higher proportion of radiogenic elements (potassium, uranium and thorium) compared with the sand. Hamilton, et al. (2014) defined a set of lithofacies for the Surat Basin using density and gamma values based on well log analysis. Although the entire Surat Basin stratigraphy was used in the defining of lithofacies, their investigation focused on using density and gamma logs to quantify distribution of sand, shale and coal throughout the Walloon Coal Measures.

Mathematical methods can be applied to well logs to make indirect estimations of formation properties. For example, Cosenza, et al. (2014) used linear regression analysis of sonic, magnetic resonance and X-ray diffraction (XRD) data to estimate clay content in a sedimentary sequence.

Various well logging techniques can be used to generate a theoretical composition, both in terms of elements and minerals, for targeted formations. One example of this is the Schlumberger Lithoscanner, which uses gamma ray spectroscopy to compute formation composition. An active neutron source is used to generate gamma rays through inelastic scattering and thermal neutron capture, which are then detected by the tool. Interpretation of the detected gamma ray spectrum is used to compute element weight fractions and mineralogy (Radtke, et al. 2012).

Here we investigate the hypothesis that potassium free or low-potassium clay minerals are the dominant clay minerals in the Springbok Sandstone, and review the effect this has on the ability of conventional well log analysis to successfully highlight high clay content rock units within the formation. A laboratory analysis program comprising mineralogy and major element analysis using drill core from within the basin provides new and detailed insight into the composition of this important formation.

METHOD AND RESULTS

Well logs and whole core photographs were reviewed to help guide core sample selection. Sample sites were identified in well logs highlighting changes in log response (gamma, density, neutron porosity, photoelectric effect) using a statistical cluster analysis. This statistical analysis is being presented in a separate presentation at the AEGC. Whole core photographs were compared with well logs, particularly FMI (Fullbore Formation Microimager) image logs to correlate core depth to log depth.

Core samples were taken by selecting an approximately 14cm long section of core, and cutting a one third slab section. Core sections were photographed post slabbing to record overall structure and appearance of sample sections (figure 2).

Core slabs were crushed and sieved to sub 1mm particle size using a hardened steel jaw crusher. A 15gram sample was separated for XRD Clay analysis. A 30 gram sample was separated, sieved and milled to sub 250 micron particle size using a tungsten carbide ring mill for XRD analysis. A 30 gram sample was separated and milled for 5 minutes in a tungsten carbide ring mill to powder sample for XRF fusion.

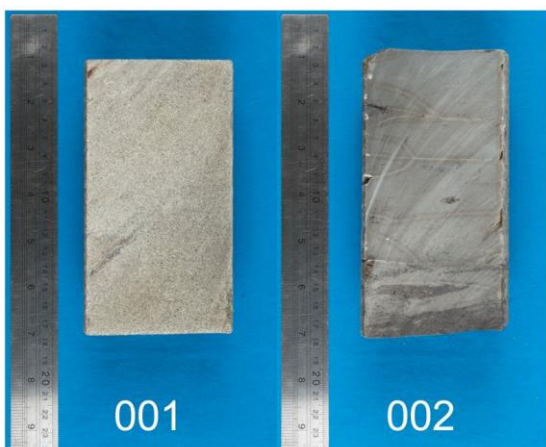


Figure 1 An example of core sections sampled from the test well, showing a sandstone and a mudstone from within the Springbok Sandstone.

Qualitative XRD clay analysis was conducted to identify clay phases present within each sampled depth interval. Quantitative XRD analysis was conducted to identify mineral phases present as weight percent of each depth interval. X-ray fluorescence (XRF) analysis was conducted on fused glass discs to analyse major element composition.

XRD analysis reveals quartz, feldspars, and various clay minerals as the dominant mineral assemblages in most samples. Montmorillonite and kaolinite clay phases have been identified throughout the formation. Kaolinite ranges from 0-18% by weight, montmorillonite from 0-88% by weight. Chlorite and muscovite have also been identified, both ranging from 0-5% throughout the formation. Selected rock composition and mineralogy results are displayed in figure 2. Siderite has also been found in some samples, including one sample greater than 45% siderite by weight. Total clay content for each sample has been calculated as the sum of weight percentages of all clay minerals (montmorillonite, kaolinite, chlorite and muscovite) reported in XRD results.

X-ray fluorescence has been used to determine major element chemistry. Results are reported as oxides. Selected oxide concentrations are displayed in figure 3. SiO_2 is the dominant oxide throughout. As total

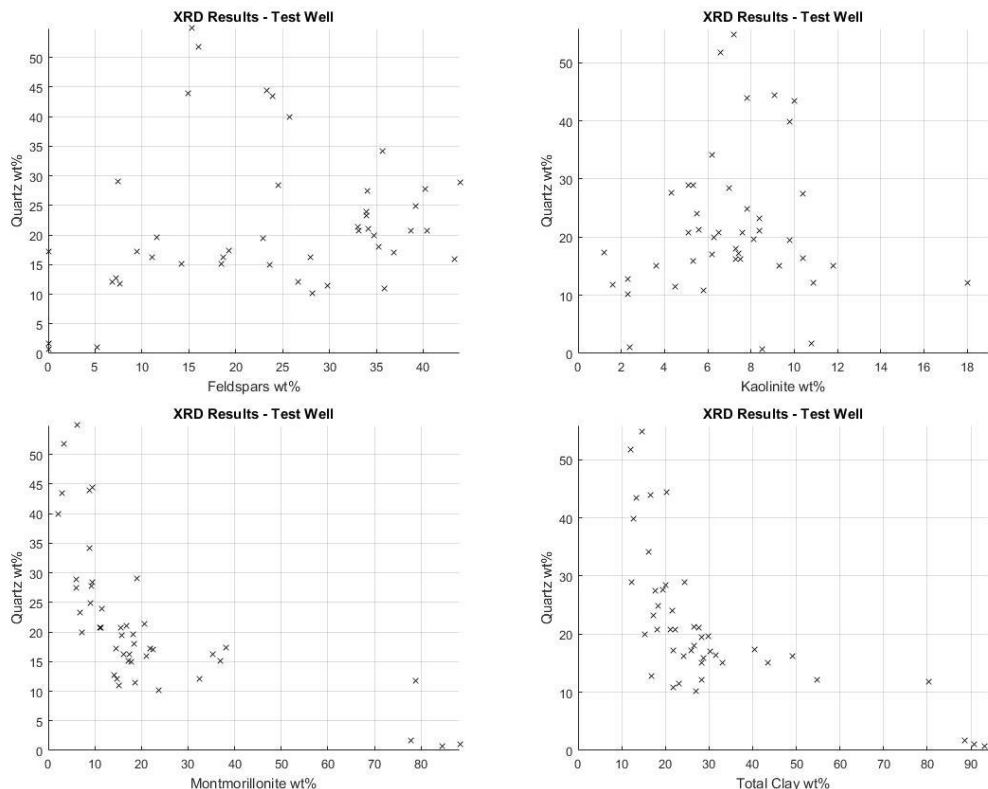


Figure 2 selected mineralogy for samples from the Test Well

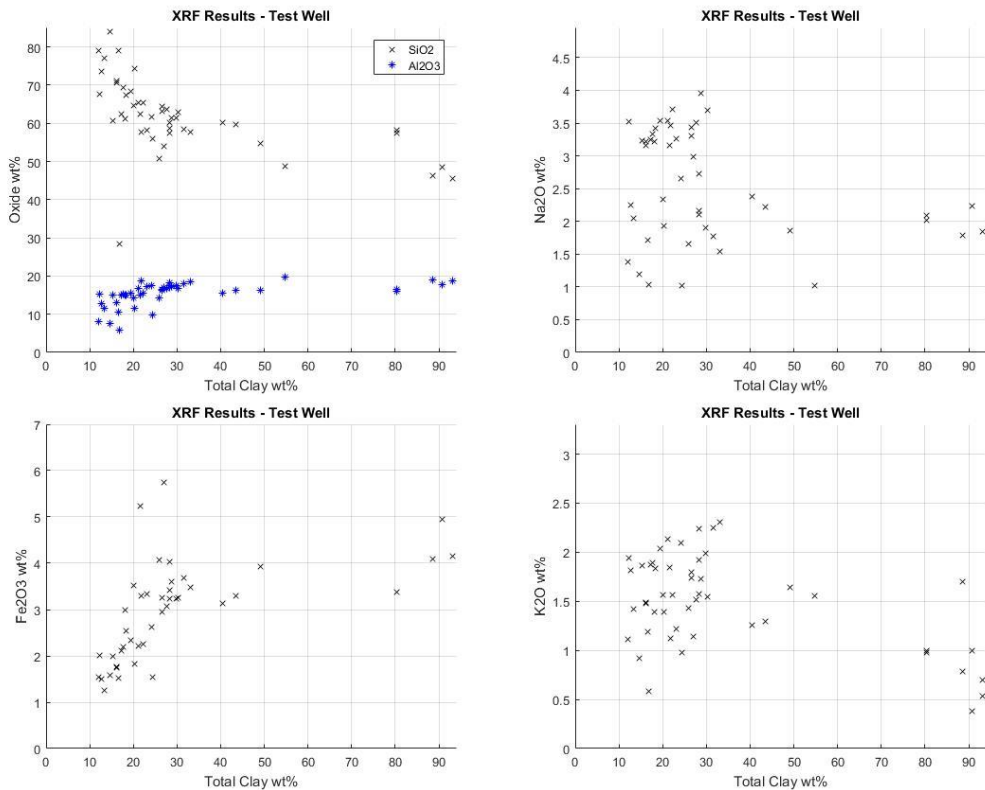


Figure 3 Comparisons of oxide abundances with total clay content

clay content is of primary importance to this research, oxides have been plotted against total clay content. Samples with a high siderite content have a corresponding high iron content. Two samples have siderite of 8.1% and 48.9%, and Fe₂O₃ content of 10.2% and 37.5% respectively. These samples are not shown in figure 3. Of particular interest is the potassium measured throughout the formation. Figure 3 demonstrates that high clay content samples (clay>80%) do not show higher potassium content than lower clay samples, and in many cases show lower potassium than many lower clay (<30%) samples.

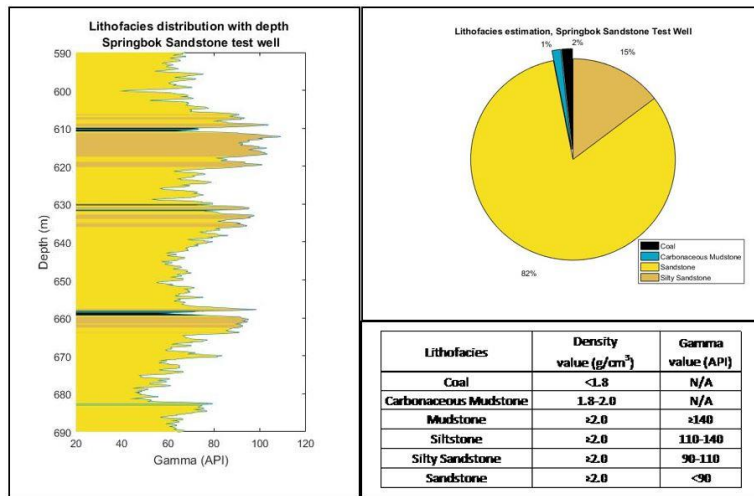


Figure 4 Lithofacies classification for Springbok Sandstone within test well. Lithofacies cutoff values after Hamilton, et al. (2014)

Well logs from the test well have been used to generate a lithofacies distribution and abundance in figure 4. Lithofacies abundances are 82% “sandstone” and 15% “silty sandstone”. There are no depth intervals in the formation which are identified as “siltstone” or “mudstone” by this analysis.

Figure 5 shows comparisons of well log data to laboratory data. Routinely used well logs (gamma, neutron density, neutron porosity and photoelectric factor) have been compared to total clay content. In addition to these logs, the Schlumberger Lithoscanner tool was run in this well. Element concentrations reported by the lithoscanner are compared with XRF data in figure 6. The element concentrations are reported as element percentages, not as oxides. The XRF data has been adjusted accordingly.

The processed lithoscanner data includes mineralogy estimates. Figure 7 compares the lithoscanner mineralogy estimates with the laboratory measurements.

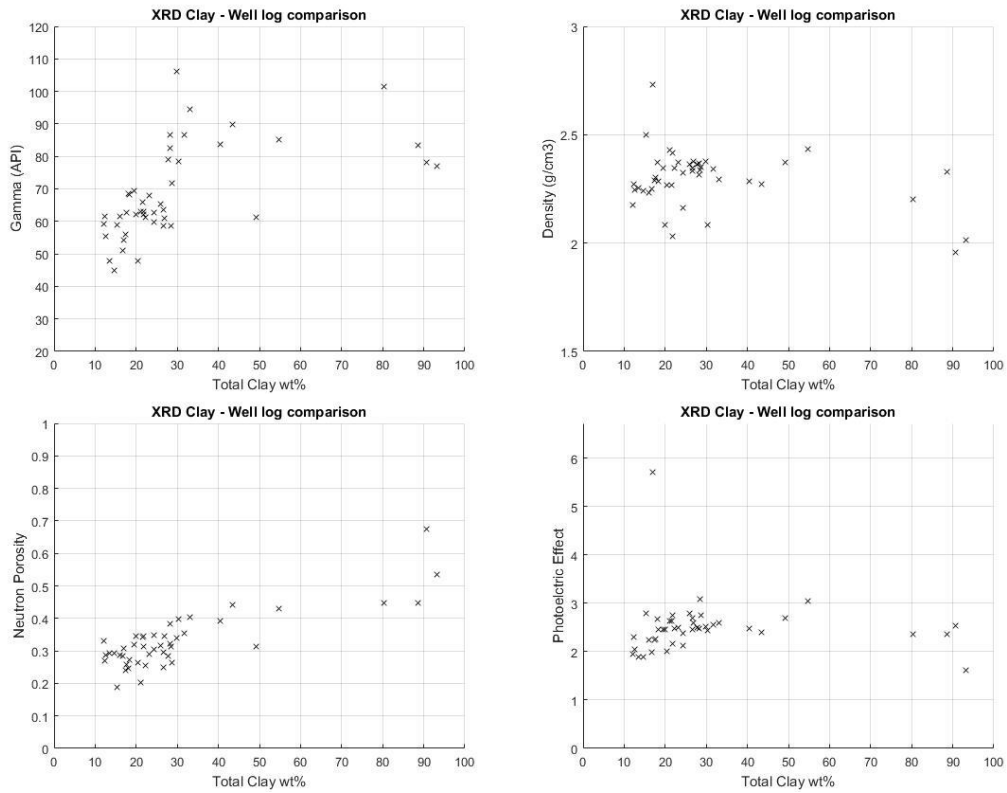


Figure 5 Total clay content compared with well log measurements

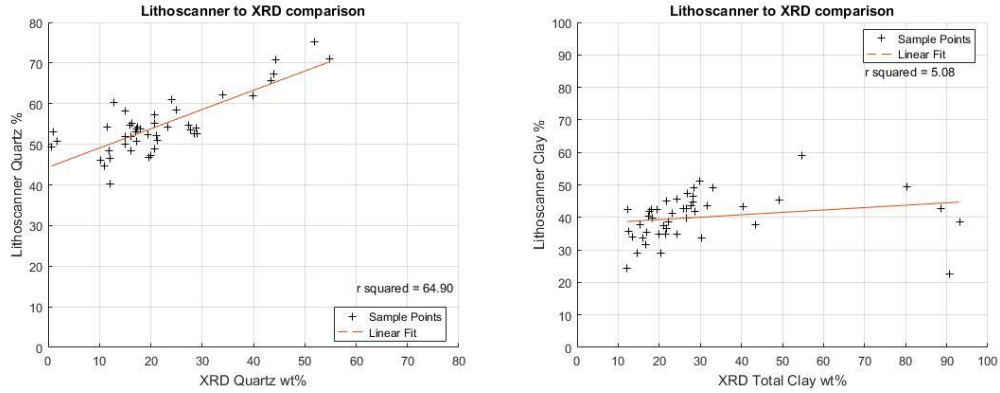


Figure 6 Lithoscanner mineralogy data compared with laboratory measurements

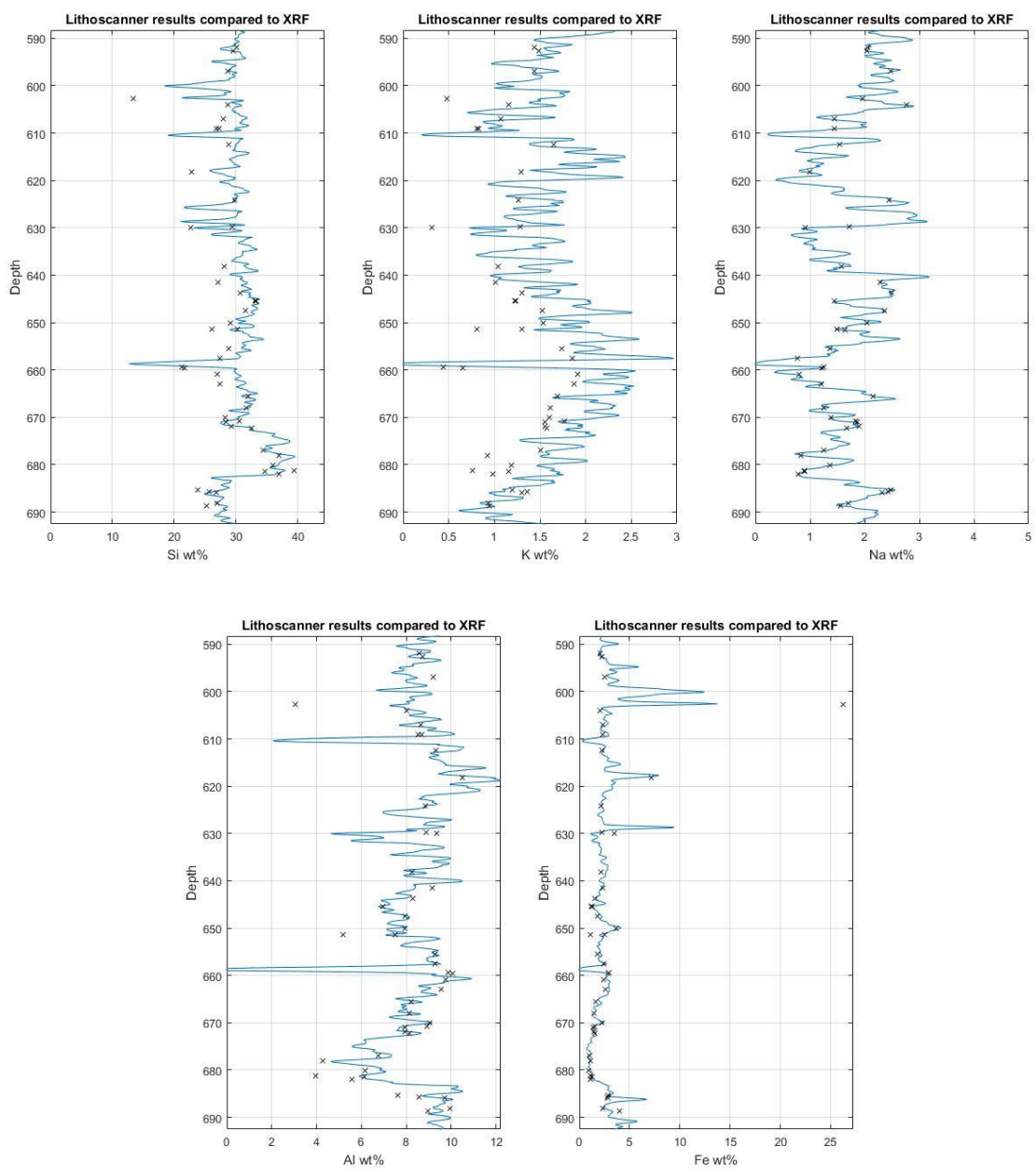


Figure 7 Lithoscanner element data compared with laboratory measurements

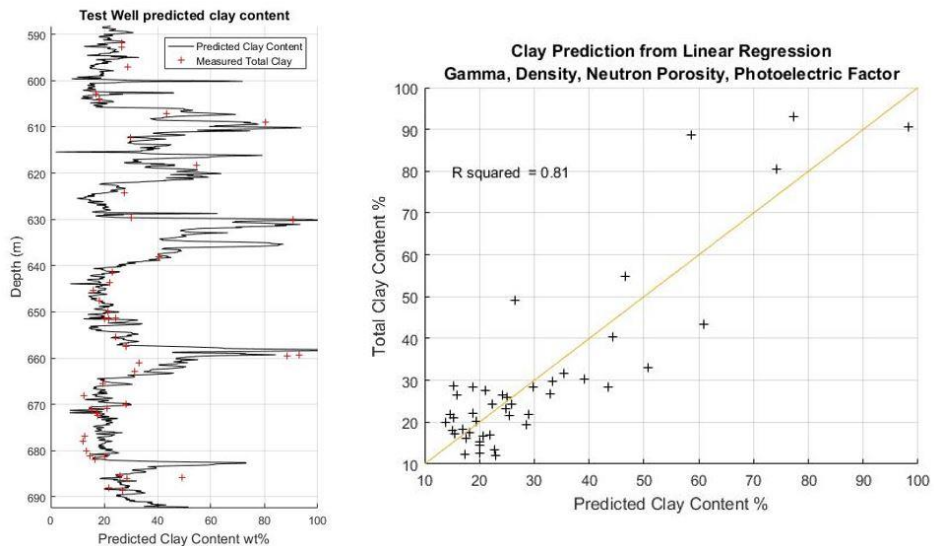


Figure 8 Total Clay prediction using linear regression model based on well logs.

Linear regression has been used to combine multiple well log measurements into a predictive model for total clay content. Well logs used for this regression are Gamma, Neutron Density, Neutron Porosity and Photoelectric Factor, and the model is based on the laboratory measured total clay values. The results of this regression are shown in figure 8. Using this predicted clay content, we define a new set of lithofacies for the formation (figure 9).

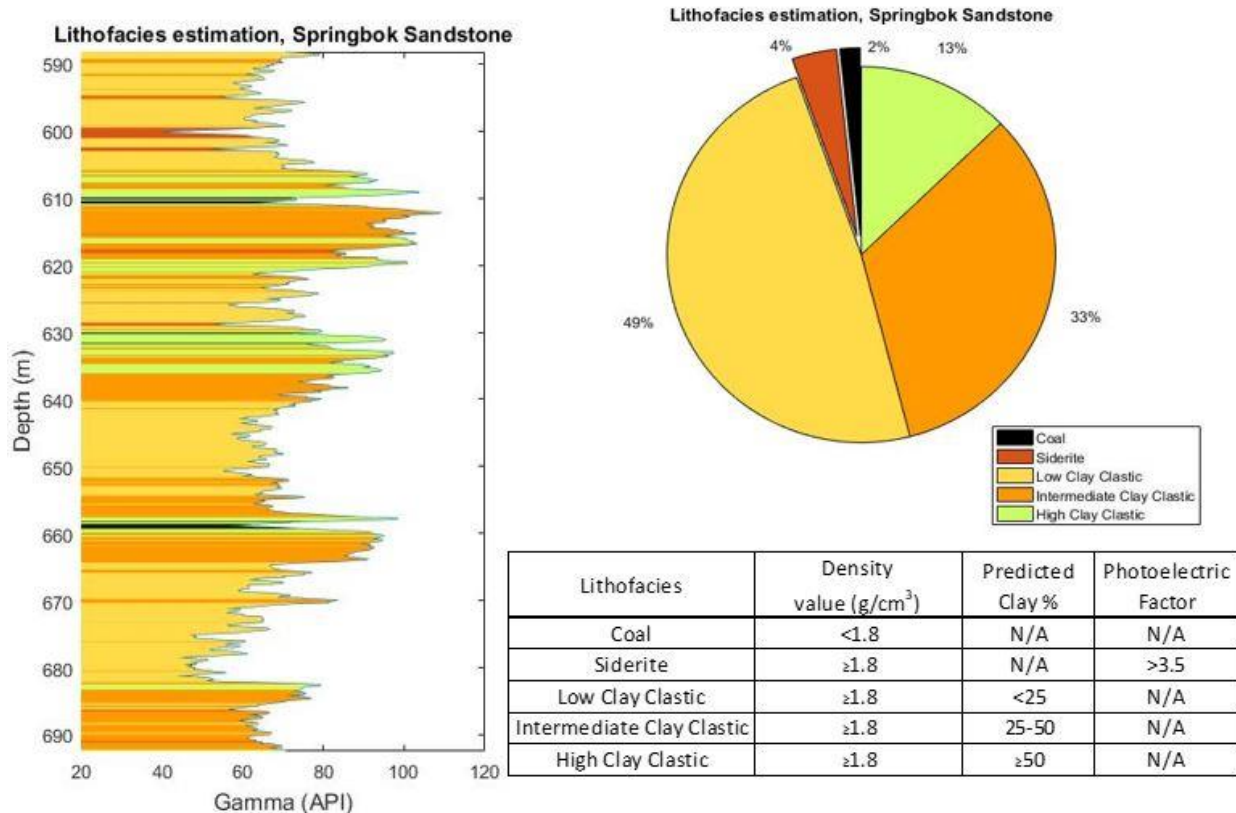


Figure 9 Lithofacies classification for Springbok Sandstone within test well using density and photoelectric well logs, and a predictive model for clay content

CONCLUSIONS

Figure 2 shows that montmorillonite and kaolinite are the dominant clay minerals within the sampled sections of the Springbok Sandstone. These clays are both typically low in potassium and high in aluminium compared to generally more potassium rich illite clays (Ellis 2007). Montmorillonite and total clay content show a general trend of increase as quartz content decreases, however such a trend is not present for kaolinite. While figure 3 shows a weak correlation between increasing clay content and decreasing SiO₂ content, trends in other oxide concentrations compared with clay content are less apparent. High Fe₂O₃ concentrations are consistent with the presence of siderite in some samples. There does not appear to be any significant increase in potassium content of samples with increasing clay content. Some of the highest clay samples have lower percentages of potassium when compared to samples with less than 30% clay.

Gamma log values compared to clay content are shown in Figure 5. There are three samples with total clay content higher than 85% which have a corresponding gamma log response of less than 90 API. Samples with a total clay content between 25% and 35% have corresponding gamma values between 57 and 107 API.

Figure 5 shows photoelectric effect may be a useful measure in identifying samples with high siderite content. This can be seen by the sample with 48.9% siderite corresponding to a photoelectric effect of 5.72, in contrast to the remainder of the dataset ranging from 1.63 to 3.09. There is no clear trend in the photoelectric effect log to differentiate high clay from low clay rocks in the Springbok Sandstone. High siderite samples correspond to densities higher than 2.7kg/m³, however no clear trend is evident in the remaining dataset which easily differentiates low and high clay samples. Samples with a higher clay content appear to have a higher neutron porosity log value.

A comparison has been made between element concentrations reported by the Schlumberger Lithoscaner and the laboratory results (figure 7). Major element concentrations generally show good correlation between the measured samples and the Lithoscaner data. The Lithoscaner data slightly overestimates K concentration, but there is still good agreement between the log values and the laboratory measurements. The high siderite sample has an Fe concentration of 26.24%. The Lithoscaner underestimates this concentration at 7.7%, however the rest of the dataset correlates well with the laboratory analysis, however the highest iron peaks in the log data does coincide with the high siderite samples. Overall, the major element concentrations from the Lithoscaner correlate well with the laboratory analysis.

The mineralogy dataset from the Lithoscaner is generated using proprietary algorithms to model mineralogy based on element concentrations. Figure 6 shows a comparison between quartz content and total clay content for the Lithoscaner data and laboratory XRD data. The Lithoscaner consistently overestimates quartz content throughout the formation. Clay content is estimated poorly by the Lithoscaner, overestimating clay content in clay poor samples and underestimating clay content in high clay samples, with an overall poor agreement between the two datasets.

Wireline lithofacies interpretation from Hamilton, et al. (2014) has been applied to the wireline logs from the test well (Figure 4). Despite high clay content (>80% clay) samples having been identified and sampled from the well, the cutoff values used do not appear to highlight high clay content rocks well within this formation. Using additional well logs we have generated a predictive model for total clay content using linear regression (figure 9). When compared to figure 4, this new lithofacies model appears to better characterise the variations in composition throughout the formation.

These results appear to confirm the hypothesis that low potassium clay minerals are the dominant clay phases throughout the Springbok Sandstone. Conventional well log analysis using gamma logs appear to be insufficient in identifying clay rich rocks throughout the formation due to the low potassium content of the dominant clay phases. Active neutron logging tools show promise in being able to identify lithologies within the formation. Although there is good agreement between the element concentrations reported by the Lithoscaner tool and the laboratory analysis, the fitting algorithm and interpretation which has been applied to the Lithoscaner dataset in this case has not provided a reliable estimate of mineralogy, particularly with regard to the total clay content of the formation. Using a model to predict clay content from multiple well logs (gamma, density, neutron porosity and photoelectric factor), a lithofacies model is demonstrated which appears to identify changes in lithology in greater detail than previous analysis which relies on gamma logs alone.

REFERENCES

- Cosenza, P., Robinet, J.C., Prêt, D., Huret, E., Fleury, M., Géraud, Y., Lebon, P., Villiéras, F., and Zamora, M., 2014, Indirect Estimation of the Clay Content of Clay-Rocks Using Acoustic Measurements: New Insights from the Montiers-Sur-Saulx Deep Borehole (Meuse, France). *Marine and Petroleum Geology* **53**, 117-32.
- Ellis, D.V., 2007, *Well Logging for Earth Scientists*. Springer Netherlands.
- Exon, N.F., 1976, *Geology of the Surat Basin in Queensland / N.F. Exxon*. Australian Govt. Pub. Service.
- Hamilton, S.K., Esterle, J.S., and Sliwa, R., 2014, Stratigraphic and Depositional Framework of the Walloon Subgroup, Eastern Surat Basin, Queensland. *Australian Journal of Earth Sciences* **61**, 1061-80.
- Hodgkinson, J. and Grigorescu, M., 2012, Background Research for Selection of Potential Geostorage Targets—Case Studies from the Surat Basin, Queensland. *Australian Journal of Earth Sciences* **60**, 71-89.
- Hoffmann, K.L., Totterdell, J.M., Dixon, O., Simpson, G.A., Brakel, A.T., Wells, A.T., and McKellar, J.L., 2009, Sequence Stratigraphy of Jurassic Strata in the Lower Surat Basin Succession, Queensland. *Australian Journal of Earth Sciences* **56**, 461-76.

- Korsch, R.J. and Totterdell, J.M., 2009, Evolution of the Bowen, Gunnedah and Surat Basins, Eastern Australia. *Australian Journal of Earth Sciences* **56**, 271-72.
- Radtke, R.J., Lorente, M., Adolph, B., Berheide, M., Fricke, S., Grau, J., Herron, S., Horkowitz, J., Jorion, B., Madio, D., May, D., Miles, J., Perkins, L., Philip, O., Roscoe, B., Rose, D., and Stoller, C., 2012, A New Capture and Inelastic Spectroscopy Tool Takes Geochemical Logging to the Next Level. Society of Petrophysicists and Well-Log Analysts.